Zeolites

Dimethyl Carbonate in the Supercages of NaY Zeolite: The Role of Local Fields in Promoting Methylation and Carboxymethylation Activity**

*Francesca Bonino, Alessandro Damin, Silvia Bordiga, Maurizio Selva, Pietro Tundo, and Adriano Zecchina**

In the last two decades the need for safer processes has focused a great deal of attention on the use of small organic carbonates, especially dimethyl carbonate ($MeOCO_2Me$: DMC). DMC is a nontoxic compound that can profitably

[*] Dr. F. Bonino, Dr. A. Damin, Prof. Dr. S. Bordiga, Prof. Dr. A. Zecchina
Department of IFM Chemistry and
NIS Centre of Excellence
Università di Torino
Via P. Giuria 7, 10125 Torino (Italy)
Fax: (+39) 011-670-7855
E-mail: adriano.zecchina@unito.it
and
INSTM
UdR di Torino (Italy)
Prof. Dr. M. Selva, Prof. Dr. P. Tundo
Department of Environmental Science
Università Ca'Foscari
Dorsoduro 2137, 30123 Venezia (Italy)
and
Interuniversity Consortium "Chemistry for the Environment"
UdR di Venezia (Italy)

[**] This project was supported by COST Action D29.

Supporting information for this article is available on the WWW under http://www.angewandte.org or from the author.

  DOI: 10.1002/ange.200500110

replace very harmful methyl halides (or dimethyl sulfate) and phosgene in both methylation and carboxymethylation processes.[1] In recent times it has been observed that methylation of primary aromatic amines with DMC is efficiently catalyzed by alkali-metal-exchanged faujasites (e.g. NaY). The peculiarity of the process is that DMC-mediated methylation of amines proceeds with unprecedented monomethyl selectivity (up to 99%) and complete chemoselectivity at the amino group in the case of ambident nucleophiles. Another peculiarity of NaY is that it also catalyzes carboxymethylation reactions. These findings suggest that under the appropriate conditions the DMC/NaY interaction leads to weakening (activation) of both $O-CH_3$ and $C-OCH_3$ bonds. The discovery of highly selective catalysts for reactions involving DMC is of special interest from both environmental and synthetic standpoints because it offers important and innovative protocols for the synthesis of high-value-added pharmaceutical intermediates and dyestuffs.[2]

It has been reasonably hypothesized that activation of DMC in the restricted spaces of the internal cavities (supercages) of NaY occurs by an electric-field-induced polarization of the molecule, which is accompanied by elongation and weakening of the $O-CH_3$ and/or $C-OCH_3$ bonds. To clarify this fundamental point, the aim of this investigation is to shed light on the structural perturbation induced in DMC upon interaction with the positively charged counterions present in the supercages. For this purpose a study of the modification of the IR properties of DMC, induced by the interaction with NaY, has been performed; the experimental results obtained are compared with ab initio simulations. It will be shown that the interaction of DMC with Na^+ ions fully explains why NaY is so effective in promoting the methylation and carboxymethylation activity of DMC.

This spectroscopic investigation takes advantage of the fact that, as DMC is a liquid, it can be easily dosed from the gas phase onto activated NaY and that, upon diffusion inside the pores, the IR spectrum of DMC can easily be recorded in situ.[3]

The available frequency range for the IR study on NaY ($\tilde{\nu} > 1300\ cm^{-1}$) only allows the observation of the $\nu(CO)$ mode of the $C-O_1$ bond (see Figure 1a), the $\nu_{asymm.}(CO_2)$ mode of the O_2-C-O_3 moiety (see Figure 1b), and the $\delta(CH_3)$ modes of the methyl groups. The bands associated with $\nu_{symm.}(CO_2)$, $\nu_{symm.}(O-CH_3)$, and $\nu_{asymm.}(O-CH_3)$, which would be of high diagnostic utility, cannot be observed because they fall within the zeolite framework region.

The dashed line in Figure 2a represents the background-subtracted spectrum of DMC completely filling the supercages (DMC/$Na^+ > 1$) (obtained by equilibration at the vapor pressure of DMC). Under these conditions the spectrum is characterized by broad and complex absorptions in both the $\nu(CO)$ (1805–1710 cm^{-1}) and $\nu_{asymm.}(CO_2)$ (1340–1235 cm^{-1}) ranges due to the superposition of the contributions from DMC interacting directly with the cations of the walls and liquid-like DMC filling the residual spaces of the supercages. Because of this multiple contribution, this spectrum is of little utility.

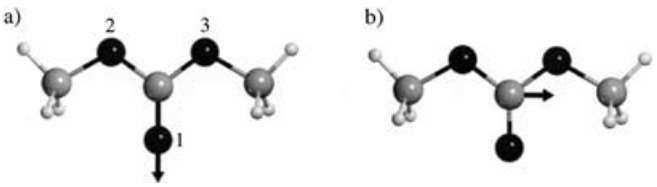

Figure 1. Pictorial representation of the normal modes of DMC1: a) $\nu(CO)$; b) $\nu_{asymm.}(CO_2)$. White spheres: H atoms; gray spheres C atoms; black spheres: O atoms.

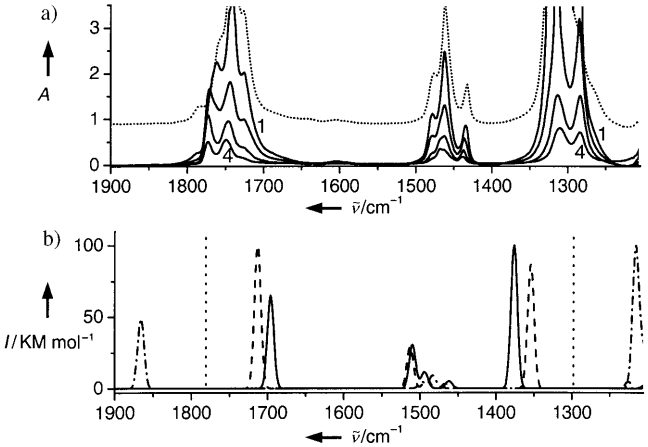

Figure 2. a) Dashed line: background-subtracted spectrum of vapor pressure of DMC on NaY zeolite outgassed at 673 K. Curves 1–4: effect of progressive outgassing at 353, 393, 423, and 453 K respectively. b) Computed IR spectra of structures **b**, **c**, and **d** reported in Figure 4. Dotted lines correspond to the computed spectrum of the DMC1 isomer.

To reveal the contribution of DMC in direct contact with the Na^+ ions present on the walls, we removed the liquid-like fraction by controlled desorption and collected a series of spectra corresponding to decreasing DMC/Na^+ ratios (curves 1–4, solid lines in Figure 2a). It can be seen that, after removal of liquid-like DMC, the $\nu(CO)$ and $\nu_{asymm.}(CO_2)$ modes clearly split into two major components at 1772–1747 and 1311–1284 cm^{-1}, respectively, while the bending frequencies of the methyl groups are essentially unaffected. The half-width of the components of the 1747–1311 cm^{-1} pair is larger than that of the 1772–1284 cm^{-1} pair, which suggests that they are caused by a family of similar species, instead of a single one. A shoulder is also observable at 1728 cm^{-1}. The relative intensity of the doublets' components changes with coverage, which allows us to conclude that the 1772–1284 and the 1747–1311 doublets belong to two different species (I and II, respectively). For the reasons described above, species II has a composite structure. A relevant observation concerning the species I and species II pairs is that the frequency difference $\Delta\nu$ between the $\nu(CO)$ and $\nu_{asymm.}(CO_2)$ modes is such that $\Delta\nu_I > \Delta\nu_{gas} > \Delta\nu_{II}$. This observation will be of great utility for comparison with the theoretical results (see below). In conclusion, from the IR spectroscopic data we can infer that the interaction of DMC with the Na^+ ions present in the supercages induces a relevant perturbation of the molecule, which influences the vibrational properties, and hence the force constants, of bonds with C–O character. On the basis of these results, it was not possible to advance an unambiguous

structural interpretation of the observed vibrational perturbations. Consequently, B3-LYP calculations of the structural, energetic, and vibrational features of model Na^+/DMC adducts were performed. To this end both *cis–cis* and *cis–trans* DMC structures (hereafter DMC1 and DMC2, respectively; see stick-and-ball representations in Figure 3) were

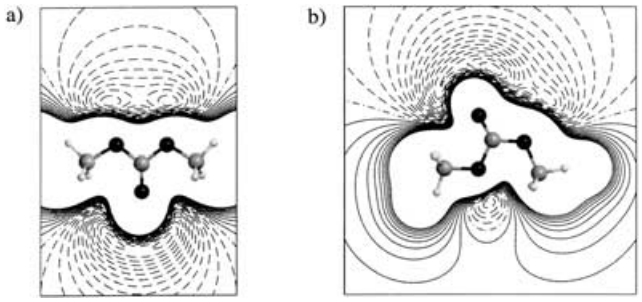

Figure 3. Pictorial representation of the computed electrostatic potential (ESP) of a) DMC1 and b) DMC2. Solid line: ESP > 0. Dashed line: ESP < 0. White spheres: H atoms; gray spheres: C atoms; black spheres: O atoms.

considered because they are very similar from the stability point of view (DMC2 being less stable by only about 12.9 kJ mol^{-1}), and hence they could be both present in the supercages as the result of an isomerization process. The computational scheme adopted (see Experimental Section for further details) is fully appropriate for this type of computation because the geometry and vibrational frequencies obtained for the DMC1 conformer are in agreement with the experimental observations.[4,5] The analysis of the molecular electrostatic potential (ESP) of DMC1 and DMC2 is shown in Figure 3, and reveals that: 1) DMC1 possesses two distinct nucleophilic sites (ESP < 0) on the oxygen of the C–O_1 bond and on the oxygen atoms of the O_2–C–O_3 moiety, and 2) DMC2 has only one nucleophilic site on the C–O_1 bond. On this basis three different DMC adducts with the complete series of naked alkali-metal cations were considered (Figure 4, structures **b**, **c**, and **d**). Such an approach has been demonstrated to be able to describe the electrostatic origin of

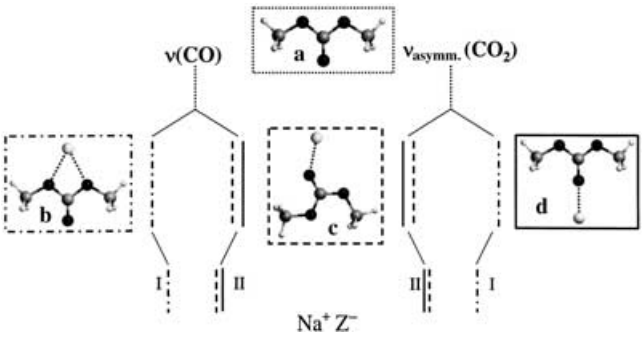

Figure 4. Vertical lines represent schematically ν(CO) and $\nu_{asymm.}(CO_2)$ of DMC under different conditions. Gas phase: isomer **a** top part; adducts **b**, **c**, and **d** middle part; experimental values obtained for NaY bottom part. The models are represented as sticks and balls with the same color code used in Figure 3. Na^+ ions in clusters **b**–**d** are represented as white spheres.

the interaction between the CO molecule and counterions in exchanged zeolites.[6] A subsequent article[7] has shown that the presence of the $AlH(OH)_3^-$ counteranion does not substantially change the conclusions reached in reference [6]. The stabilities of the adducts, as evaluated by binding energy calculations (DMC1 taken as reference reactant, BSSE accounted for),[8] are in the order **c** > **d** > **b**. As shown in Figure 5a, there is a linear correlation (positive slope)

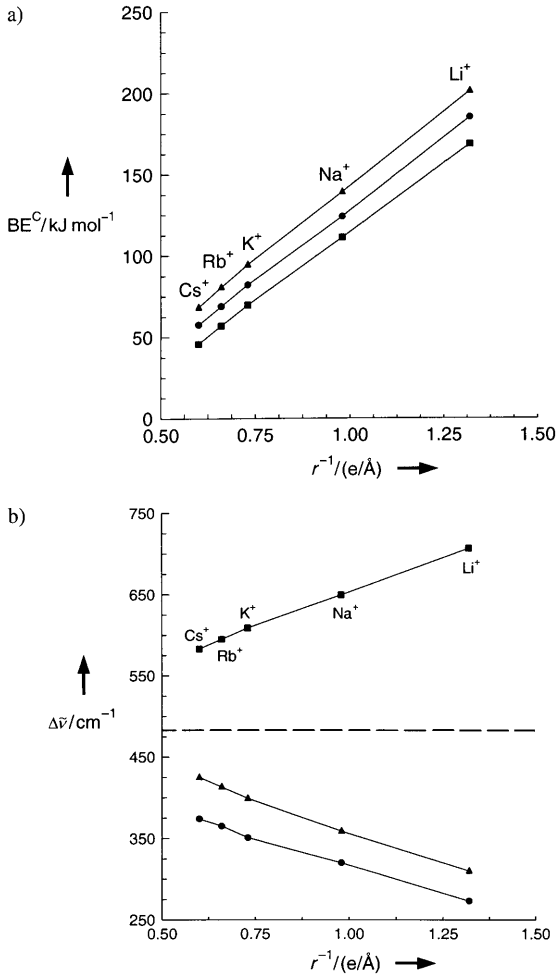

Figure 5. a) Computed BE^c (binding energy corrected for the BSSE) versus the charge density of the interacting alkali-metal cations. (■), (▲), and (●) refer to adducts **b**, **c**, and **d**, respectively. b) Computed Δν (ν(CO) − $\nu_{asymm.}(CO_2)$) versus the charge density of the interacting alkali-metal cations. (■), (▲), and (●) refer to adducts **b**, **c**, and **d**, respectively.

between the computed binding energy for the three adducts and the charge density (i.e. the reciprocal of the ionic radius for monovalent cations), thus confirming the pure electrostatic origin of the interaction. When the interaction occurs through the oxygen of the C–O_1 moiety (structures c and d in Figure 4), the calculations predict an elongation (weakening) of the C–O_1 and the $O_{2/3}$–CH_3 bonds, the remaining two C–$O_{2/3}$ bonds being shortened (strengthened). When the interaction occurs through the latter two oxygen atoms (structure **b** in Figure 4), the C–O_1 moiety undergoes a shortening

(strengthening), while the $C{-}O_{2/3}$ and the $O_{2/3}{-}CH_3$ bonds undergo a lengthening (weakening). Further interesting results come from the computed frequencies of the adducts: in structures **c** and **d** of Figure 4 the ν(CO) and $\nu_{asymm.}(CO_2)$ are red- and blue-shifted, respectively, with respect to isolated DMC1, whereas in structure **b** of Figure 4 the opposite behavior is observed. The computed spectra obtained in the case of Na^+ are shown in Figure 2b and in Figure 4 as dotted (**a**), dot-dashed (**b**), dashed (**c**), and full (**d**) lines, and show that $\Delta\nu_{\mathbf{b}} > \Delta\nu_{gas} > \Delta\nu_{\mathbf{c}} \approx \Delta\nu_{\mathbf{d}}$. A similar trend is observed for the other alkali-metal cations, as shown in Figure 5b, from which it is clear that this observation also correlates with the charge density of the interacting cations.

These values are clearly in qualitative agreement with the experimental observations (reported in Figure 2a and schematized in Figure 4). Another interesting result is that structures **c** and **d** have very similar spectroscopic features and hence they behave as a family of similar species, in agreement with the observed half-width of the components of species II. Of course, the computed Δν values are higher than the experimental ones, because the model adducts involve bare Na^+ ions; in fact their polarizing power is higher than that of the Na^+ counterions in the supercage, whose positive charge is partially counterbalanced by the negative charge of the framework.

In conclusion, on the basis of a comparison of the experimental and computed data we have been able to conclude that both *cis–cis* and *cis–trans* species are present in the NaY supercages and to identify the properties of the adducts formed by these species with the Na^+ ions. In particular, the electrostatic perturbation in adducts **c** and **d** induces an elongation (weakening) of the $O{-}CH_3$ bonds, a fact which can explain the catalytic activity of NaY in methylation reactions. In adduct **b** an elongation of the $C{-}OCH_3$ occurs, which justifies the catalytic activity of NaY in carboxymethylation reactions. Finally, the observation that the IR components associated with structure **b** are the preferred ones at lowest coverage (higher evacuation temperature) could explain a different selectivity of the DMC/NaY system towards carboxymethylation reactions.

Taken together, these results afford, in a simple and direct manner, a reasonable explanation why NaY is a useful catalyst for methylation and carboxymethylation reactions with DMC. The role of polarization forces associated with the Na^+ counterions that are present in the restricted spaces of the supercages in DMC activation is also clearly demonstrated.[2c]

Experimental Section

An NaY sample (Aldrich, Si/Al ≈ 3), in the form of a thin, self-supported wafer, was activated at 673 K in vacuo (up to 10^{-5} mbar) before contact with DMC. Liquid DMC (ACROS Organics, 99% in purity) was dosed in the gas phase in a vacuum manifold directly connected to the measurement cell. IR spectra were recorded with a Bruker IFS 66 FTIR spectrometer equipped with an HgCdTe cryodetector (4000–700 cm^{-1} range) with a resolution of 2 cm^{-1}.

All calculations were performed by density functional theory procedures[9] with the B3-LYP[10] Hamiltonian, as implemented in Gaussian 98.[11] Li, Na, K, Rb, and Cs atoms were described with basis-set adopted by Ferrari et al.[6]. For C and O atoms, the fully optimized triple-ζ valence basis-set (TZV) of Ahlrichs et al.[12] was emplyed. A double set of diffuse p functions on the cations was added ($\zeta_p(Na) = 0.131$ and 0.0196 $Bohr^{-2}$). Moreover, the TZV basis sets for C and O atoms (hereafter TZV2d) were also supplemented by a double set of polarization d functions: ζ_d values were derived from the standard ones[13] following an even-tempered recipe ($\zeta_d(C) = 1.6$ and 0.4 $Bohr^{-2}$; $\zeta_d(O) = 2.4$ and 0.6 $Bohr^{-2}$). Hydrogen atoms in the DMC molecule were described by means of a standard Pople 6-311 + G(d,p) basis set.

Received: January 12, 2005
Revised: March 25, 2005
Published online: June 29, 2005

Keywords: density functional calculations · green chemistry · IR spectroscopy · methylation · zeolites

[1] a) P. Tundo, M. Selva, *Acc. Chem. Res.* **2002**, *35*, 706–716; b) Z. H. Fu, Y. Ono, *Catal. Lett.* **1993**, *22*, 277–281; c) P. R. H. P. Rao, P. Massiani, D. Barthomeuf, *Catal. Lett.* **1995**, *31*, 115–120.
[2] a) M. Selva, P. Tundo, A. Perosa, *J. Org. Chem.* **2002**, *67*, 9238–9247; b) M. Selva, P. Tundo, A. Perosa, *J. Org. Chem.* **2003**, *68*, 7374–7378; c) M. Selva, P. Tundo, *Tetrahedron Lett.* **2003**, *44*, 8139–8142.
[3] T. Beutel, *J. Chem. Soc. Faraday Trans.* **1998**, *94*, 985–993.
[4] F. C. Mijlhoff, *J. Mol. Struct.* **1977**, *36*, 334–335.
[5] H. Bohets, B. J. van der Veken, *Phys. Chem. Chem. Phys.* **1999**, *1*, 1817–1826, and references cited therein.
[6] A. M. Ferrari, P. Ugliengo, E. Garrone, *J. Chem. Phys.* **1996**, *105*, 4129–4139.
[7] A. M. Ferrari, K. M. Neyman, N. Rösch, *J. Phys. Chem. B* **1997**, *101*, 9292–9298.
[8] G. Lendvay, I. Mayer, *Chem. Phys. Lett.* **1998**, *297*, 365–373.
[9] a) P. Hohenberg, W. Kohn, *Phys. Rev.* **1964**, *136*, B864–B871; b) W. Kohn, L. J. Sham, *Phys. Rev.* **1965**, *140*, A1133–A1138.
[10] a) C. Lee, W. Yang, R. G. Parr, *Phys. Rev. B: Condens. Matter* **1988**, *37*, 785–789; b) A. D. Becke, *J. Chem. Phys.* **1993**, *98*, 1372–1377; c) A. D. Becke, *J. Chem. Phys.* **1993**, *98*, 5648–5652.
[11] Gaussian 98, Revision A.11, M. J. Frisch et al., see Supporting Information.
[12] A. Schafer, C. Huber, R. Ahlrichs, *J. Chem. Phys.* **1994**, *100*, 5829–5835.
[13] A. Schafer, H. Horn, R. Ahlrichs, *J. Chem. Phys.* **1992**, *97*, 2571–2577.

